C. R. Palevol 10 (2011) 357–366

Contents lists available at ScienceDirect

Comptes Rendus Palevol

www.sciencedirect.com

General palaeontology, systematics and evolution (Taphonomy and fossilisation)

Analysis of fossil bone organic matrix by transmission electron microscopy

Analyse de la matrice organique d'os fossiles par microscopie électronique à transmission

Louise Zylberberg [a,*], Michel Laurin [b]

[a] *UMR 7193, ISTEP, équipe biominéralisations et paléoenvironnements, université Pierre-et-Marie-Curie, 4, place Jussieu, BC19, 75252 Paris cedex 05, France*
[b] *UMR 7207, CNRS/MNHN/UPMC, "centre de recherches sur la paléobiodiversité et les paléoenvironnements", Muséum national d'histoire naturelle, département histoire de la Terre, bâtiment de géologie, case postale 48, 43, rue Buffon, 75231 Paris cedex 05, France*

ARTICLE INFO

Article history:
Received 14 December 2010
Accepted after revision 5 April 2011
Available online 28 June 2011

Written on invitation of the Editorial Board.

Keywords:
Collagen
Fossil bone
Vertebrates
TEM
Palaeohistology

ABSTRACT

A transmission electron microscope (TEM) study was initiated on samples of geological ages ranging from Devonian to Jurassic to analyse the ultrastructure of the organic matrix in fossil bones that have preserved a histological structure after demineralisation. All samples show a network of variably well-preserved fibrils. Within the sampling, the best results were obtained in two specimens: the scales of the Devonian sarcopterygian tetrapodomorph *Eustenopteron foordi*, and the humerus of Jurassic dinosaur *Lappentosaurus madagascariensis*. Despite an extended time difference between both specimens, their fossil bone is composed of a plywood-like structure in which the fibrils are very closely packed. These observations support the hypothesis that dense initial packing of collagen fibrils favours the preservation of the fossil bone.

Mots clés :
Collagène
Os fossile
Vertébrés
MET
Paléohistologie

RÉSUMÉ

L'étude ultrastructurale de la trame organique persistant après déminéralisation a été réalisée au microscope électronique à transmission sur des os fossiles dont l'âge varie du Dévonien au Jurassique. Les échantillons retenus présentent un réseau composé de fibrilles plus ou moins bien conservées. Les meilleurs résultats obtenus concernent les écailles du sarcoptérygien tétrapodomorphe *Eustenopteron foordi* datant du Dévonien et l'humérus du dinosaure *Lappentosaurus madagascariensis* datant du Jurassique. Ces deux spécimens distants par l'âge possèdent tous deux des os fossiles formés par une structure en contreplaqué : une organisation spatiale où les fibrilles de collagène sont très proches les unes aux autres et reliées entre elles. Les résultats obtenus montrent que les os fossiles les plus compacts ont une trame organique mieux préservée du point de vue ultrastructural, ce qui plaiderait en faveur de l'hypothèse du rôle de la densité osseuse comme facteur intrinsèque favorisant la préservation des os fossiles.

* Corresponding author.
E-mail address: louise.zylberberg@upmc.fr (L. Zylberberg).

1631-0683/$ – see front matter
doi:10.1016/j.crpv.2011.04.004

1. Introduction

Numerous histological studies refer to remarkable preservation of fossil bone including the persistence of the birefringence pattern observed in fresh bone where it reflects the original alignment of apatite crystals with their c-axes parallel to the collagen fibrils (for a review, see Fawcett, 1994). In bone, the organic matrix (mainly collagen fibrils) and the mineral (crystals of carbonated hydroxyapatite) are interrelated, forming a complex material (Glimcher and Krane, 1968; Weiner and Traub, 1986). The intimate association of bone mineral with the organic matrix appears to protect the collagen molecules in fossil bone; conversely, collagen provides protection for hydroxyapatite crystals so that bone hydroxyapatite crystals and collagen fibrils ensure a mutual protection affording a greater stability to both components in fossil remains (Collins et al., 1995, 2002; Eglinton and Logan, 1991; Trueman and Martill, 2002; Trueman et al., 2008).

Ultrastructural analyses using transmission electron microscope (TEM) have usually been carried out for studying extant osseous tissues; this technique is not commonly done for fossil bone. TEM analyses of well-preserved fossil bone have shown that collagen molecules (mostly type I collagen) can be preserved down to the ultrastructural level (Armitage, 2001; Doberenz and Wickoff, 1967; Isaacs et al., 1963; Pawlicki, 1985; Pawlicki et al., 1966; Rimblot-Baly et al., 1995; Shackleford and Wickoff, 1964; Zylberberg et al., 2010; Zocco and Schwartz, 1994). Most of these electron microscope studies were carried out on replicas, even those using a TEM. Thus, demineralisation of the samples was not necessary.

Other ultrastructural studies reporting the presence of collagen concern fossils often dating from the Pleistocene (Armstrong et al., 1983; Jans et al., 2002; Shackleford and Wickoff, 1964). Although collagen molecules in fossils may remain structurally intact for a long time, there is now evidence of subtle degradation that depends not only on intrinsic factors such as composition and spatial organisation, but also on extrinsic factors such as soil pH, temperature, burial conditions, and postdepositional history (i.e. Fernández-Jalvo et al., 2002; Jans et al., 2002; Schweitzer et al., 2008).

Given that type I collagen is the main component (from 90 to 95%) of the bone organic matrix (Robey, 2002), a brief review of its structure and composition may be useful. Type I collagen is a fibrillar protein that has a strong affinity for hydroxyapatite. Collagens are structural proteins of the extracellular matrix arranged into a triple helix (Rossert and de Combrugghe, 2002; Van der Rest, 1991). Each α chain contains an obligatory amino-acid sequence Glycine-X-Y. Thus, every third residue is glycine, the smallest amino-acid. X corresponds to a modified amino-acid hydroxyproline. Collagen also incorporates a specific modified amino-acid hydroxylysine. Due to this particular peptide sequence, each α chain is coiled in a left-handed helix; the three α chains are twisted together to form a right-handed triple helix where Gly residues are in the centre of the triple helix. The triple helix is stabilised by intramolecular bonds and water bridges (Rossert and de Combrugghe, 2002). Type I collagen is a heterotrimer made of two identical α1(1) chains and one α2(I) chain. Type I collagen molecules aggregate by lateral packing into fibrils that present, through electron microscopic examination, the characteristic cross-striation with a repetitive axial period of about 64 nm. The axial periodicity is explained by a quarter staggering of the molecules in the fibril where they are separated from each other by a gap (Van der Rest, 1991). The initial mineral deposition occurs in the gap region of the fibril. The crystallites are thin platelets elongated along the collagen fibrils. The crystallites are regularly stacked within the fibrils. In heavily mineralised bone, the crystals can grow and contact each other to form extensive multicrystalline arrays (Weiner and Traub, 1986). According to Lees (1989), the mineralised collagen possesses unusual features that influence its diagenesis, and apatite may be bound to collagen through calcium bridges. Previous studies lead to consider that a close packing of collagen fibrils may be an intrinsic factor increasing the resistance of bone during fossilisation through the formation of hydrogen bonding and cross-linking (Eglinton and Logan, 1991).

The aim of the present study is to observe whether organic residues remain in fossil bones after demineralisation treatments appropriate to transmission electron microscopy examination. To address this problem, it was tempting to compare the ultrastructure of the organic matrix of fossil bones that differ in the spatial organisation of bone and ranging from compact twisted plywood-like structure to less compact lamellar bone. The terminology of Francillon-Vieillot et al. (1990) concerning bone histology was used in the present study. The present preliminary work reports the results obtained on samples dating from the Devonian to the Jurassic.

2. Materials

The present study was carried out on specimens dating from the Upper Devonian up to the Middle Jurassic (Fig. 1): the tetrapodomorph *Eustenopteron foordi*, (MNHM 06-615A), scale, Late Devonian (Escumenac Bay, Quebec, Canada); the seymouriamorph *Microphon exiguus* (PIN [Paleontological Institute of Moscow] 4548, lent by M. Shishkin), rib, Late Tatarian, Middle Permian (Bulanov, 2003); the temnospondyl *Onchiodon frossardi*, ventral scales, Early Permian, Buxières-les-Mines Allier, France (lent by J.-S. Steyer); a second temnospondyl, a Dissorophoide indet. (R. Reisz, private collection), femur, Early Permian, Oklahoma, U.S.A.; a third temnospondyl, *Eryosuchus garjainovi* (PIN 2865, lent by M. Shishkin), rib, Middle Triassic; a fourth temnospondyl, *Tupilakosaurus wetlugensis*, (PIN 1025, lent by M. Shishkin) rib, Early Triassic, Wetluga River, Nizhei Province; the amniote *Captorhinus aguti*, (Armand de Ricqlès, private collection) femur, Early Permian, Oklahoma U.S.A.; the sauropodomorph dinosaur *Lappentosaurus madagascariensis*, (Armand de Ricqlès private collection) humerus, Middle Jurassic, Andromany, Madagascar. The phylogeny was compiled from Laurin (1998) for the main stegocephalian taxa, Yates and Warren (2000) and Laurin and Soler-Gijón (2006) for higher-level temnospondyl relationships (both implied the same relationships between the four temnospondyl taxa),

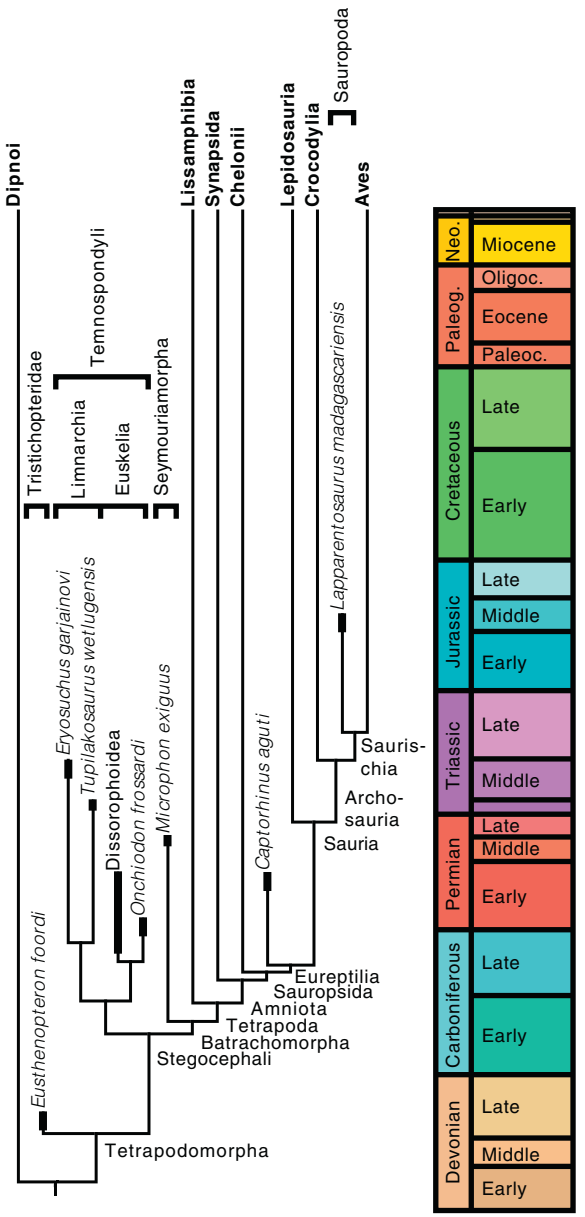

Fig. 1. Time-calibrated tree showing the stratigraphic distribution of the examined taxa. Abbreviations: Neo.: Neogene; Oligoc.: Oligocene; Paleoc.: Paleocene; Paleog.: Paleogene.

Fig. 1. Arbre calibré dans le temps montrant la distribution stratigraphique des taxons examinés. Abréviations : Neo. : Néogène ; Oligoc. : Oligocène ; Paleoc. : Paléocène ; Paleog. : Paléogène.

and Laurin and Reisz (1995) for the position of turtles. Controversies render part of this phylogeny uncertain, both concerning the position of Lissamphibia (Ruta and Coates, 2007) and of turtles (Rieppel and Reisz, 1999), but the choices that we have made are supported by recent analyses (Lyson et al., 2010; Marjanovic and Laurin, 2009). The tree was drawn using the Stratigraphic Tools (Josse et al., 2006) of Mesquite (Maddison and Maddison, 2010). The geological timescale follows Gradstein et al. (2004). Tetrapoda is considered a crown-group; for this point and other nomenclatural issues, see Laurin and Anderson (2004).

The bones display varied shades and colors indicating a range of postmortem diagenetic influences.

3. Methods

Small samples of the fossils examined in the present study were cleaned with a solution of 2.5% formic acid, rinsed in ethanol, air-dried, and embedded in Epon 812. The polymerisation was performed at 60 °C. The blocks containing the fossil samples were sectioned using an Isomet diamond saw to obtain ground sections. These ground sections are free slivers of about 10 μm thick. Some samples were not retained after examination with a light microscope of the Epon ground sections. Thus, we discarded the scales of *O. frossardi,* which are too small (Fig. 2a). We also discarded the femur of the Dissorophoidea indet. from the Early Permian, a group of terrestrial, medium-sized temnospondyl (Laurin, 2008), because ground sections do not show histological structures (Figs. 2b, c). The rib of *M. exiguus* was not retained, for the same reason. Only the samples whose demineralised ground sections showed a preserved micromorphology were submitted to further preparation for TEM examination.

Both surfaces of the ground sections selected for TEM observation were covered with a thin layer of Epon that was polymerised to prevent the breaking up of the tissues weakened during the demineralisation procedures for TEM examination. These ground sections were observed by light microscopy under natural and polarised light. The demineralising agents tested include nitric acid, hydrochloric acid, citric acid, formic acid, and ethylene diamino tetracetic acid (EDTA). The best results were obtained with organic acids and EDTA added in a fixative mixture. EDTA is a demineralising agent that has long been used for ultrastructural studies of extant osseous tissues (Hancox, 1972; Scott and Kyffin, 1978) and that has more recently been used for demineralisation of fossil calcified tissues (Armstrong et al., 1983; Schweitzer et al., 2005). The fixative solution was composed of 1.5% paraformaldehyde and 1.5% glutaraldehyde in a 0.1 M cacodylate buffer and 0.1 M citric acid or 0.5% formic acid or 5% EDTA. The demineralising solution was changed every two days for one to six months depending on the samples. The demineralisation was stopped when the samples became less opaque and more flexible. The demineralised ground sections were postfixed in a solution of 2% osmium tetroxide in the cacodylate buffer, then dehydrated in a graded series of ethanol solutions, left at least 12 hours in a 1/1 ethanol-Epon mixture and embedded in Epon. Semi-thin sections (1 μm thick) were stained with a buffered toluidine blue solution (pH 4) that revealed the presence of preserved organic matrix but did not allow discrimination between collagen and other proteins. The sections were examined by light microscopy using natural and polarised transmitted light and Nomarski differential interference contrast (DIC) to select appropriate areas for TEM examination. Ultrathin sections (100 nm thick) were stained with uranyl acetate and lead citrate and observed in a Philips

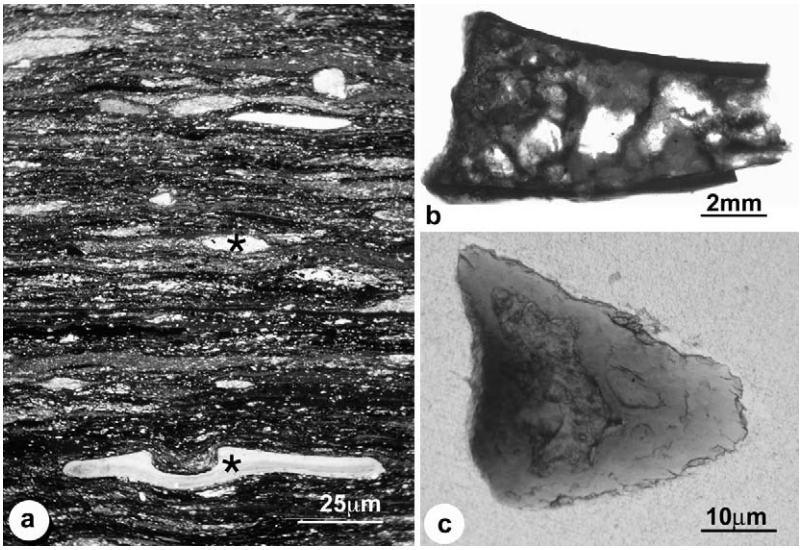

Fig. 2. Temnospondyls. (a) *Onchiodon frossardi*. Ventral scales. Ground section. Transmitted natural light. The scales distributed in the sediment are very small (asterisks). (b) Dissophorophoidea. Longitudinal section of femur. Ground section. Transmitted natural light. The cortex and the spongiosa show no structural organisation. (c) Same. Ground cross-section observed with polarised light.
Fig. 2. Temnospondyles (a) *Onchiodon frossardi*. Écailles ventrales. Lame mince. Lumière naturelle transmise. Les écailles réparties dans le sédiment sont de petite taille (astérisques). (b) Dissophorophoidea. Coupe longitudinale de fémur. Lame mince. Lumière naturelle transmise. Aucune structure n'est perceptible dans le cortex ou dans la spongiosa. (c) Même élément, coupe transversale observée en lumière polarisée.

EM 201 and a Jeol Leo TEMs with an operating voltage of 80 kV.

4. Results

4.1. Light microscopic examination.

All the fossils retained for TEM examination showed birefringent structures in mineralized ground sections observed with polarised light. However, the birefringence remained visible after demineralization, to an extent that depended on the tissue organisation and on the species.

4.2. TEM examination

The oldest fossil examined was the Devonian sarcopterygian *Eusthenopteron foordi,* whose scales were removed from slabs containing skeletal remains that show a very good preservation. Vertical sections show that the scales are composed of two layers: a superficial layer that will be described first covers the much thicker basal plate (Fig. 3a). In the present study, vertical sections refer to sections perpendicular to the skin surface. The superficial layer forms thick tubercles (Fig. 3a), as recently reported (Zylberberg et al., 2010). The basal plate is composed of superimposed plies about 10–12 μm thick (Fig. 3b). Each ply is made of closely packed parallel collagen fibres that are oriented in the same direction. The fibre direction varies from one ply to the next by a specific angle of rotation. The successive odd and even plies form a twisted plywood structure (Giraud et al., 1978; Meunier, 1984). Osteocyte lacunae are present in both layers. Cells are abundant, as observed in the sections of scales embedded in Epon for TEM observation (Fig. 3c).

These sections also show that variations of the fibril directions were preserved in sections embedded in Epon and submitted to demineralisation for TEM examination (Fig. 3c). Staining of semi-thin sections with toluidine blue indicates that organic material stained in blue is preserved within the scales, even though the scales are not completely demineralised. The mineralised areas are not stained with toluidine blue (Fig. 3d). Semi-thin sections of scales observed with Nomarski optics show abundant fractures (Fig. 3e). The basal plate has a surface covered with ripples parallel to each other (Fig. 3f).

At the ultrastructural level, long, compact structures are composed of closely packed fibrils (Fig. 3 g). Adjacent fibrils are linked to each other by regularly spaced bridges (Fig. 3 g, insert). The fibrils are about 100 nm thick, but they lack the specific striation that characterises the type I collagen fibrils present in the osseous tissues of extant vertebrates; however, a regular banding can occasionally be observed in these scales. Mineral, still present in thin sections after demineralisation procedures, forms patches associated with the fibrils (Fig. 3 h).

TEM observations were also obtained on the femur of *C. aguti,* a Permian captorhinid, a basal eureptile. The *C. aguti* femur shows a well-preserved bone organisation after demineralisation. Longitudinal ground section of the epiphyseal and metaphyseal areas show the thin cortex of compact bone surrounding the trabeculae of the central spongiosa (Fig. 4a). Numerous osteocyte lacunae (Fig. 4b_1) are seen within the matrix of the bone trabeculae made of lamellar bone (Fig. 4b_2). Semi-thin sections are stained with toluidine blue in both the cortical (Fig. 4c) and the trabecular bone (Fig. 4d). Empty osteocyte lacunae are randomly distributed. Deep blue stained rings surround circular empty spaces that most probably correspond to

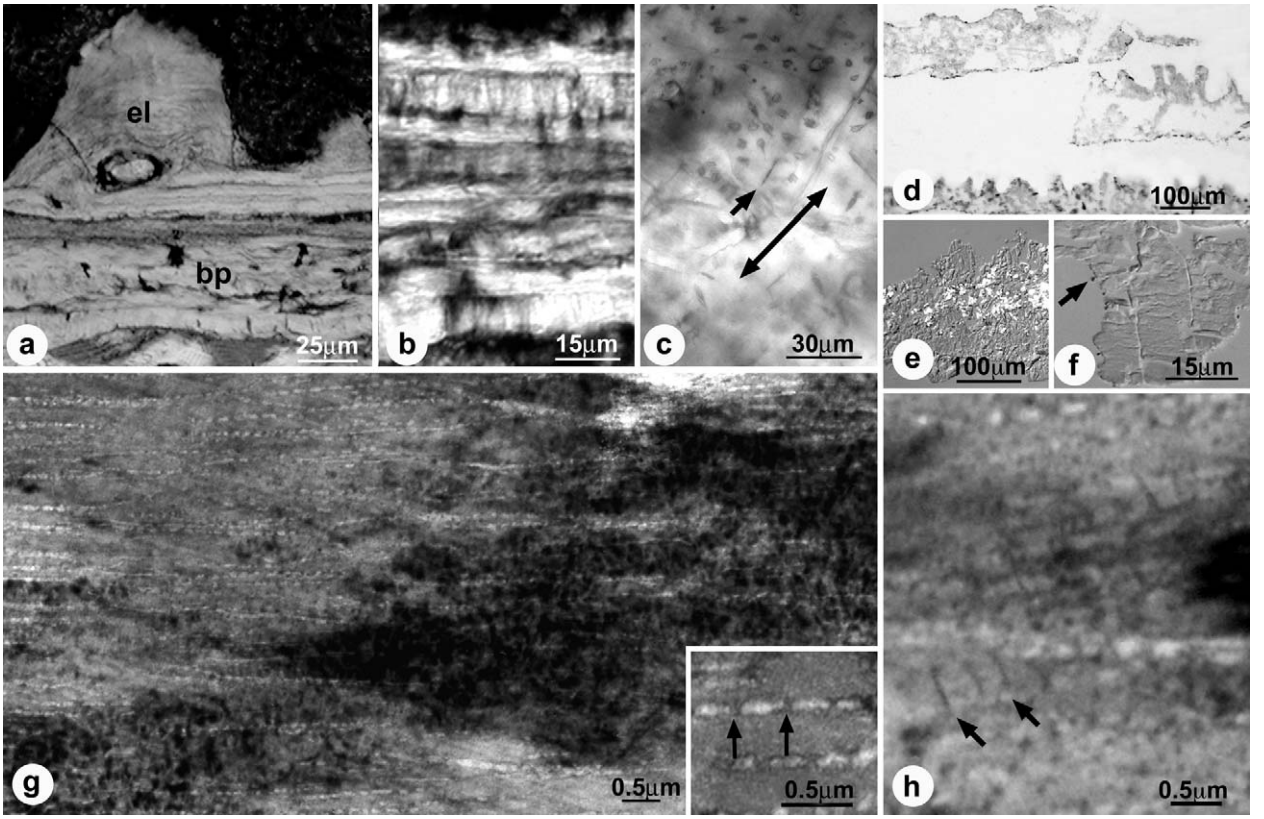

Fig. 3. *Eusthenopteron foordi* scales. (a) Transmitted natural light. Vertical ground section showing two main layers: the ridged external layer (el) and the stratified basal plate (bp). (b) Polarised light. Vertical ground section through the basal plate showing details of the superimposed plies. (c) Transmitted natural light. Epon frontal thick section after demineralisation. Note the preservation of the scale organisation. The shape of the osteocyte lacunae and their canaliculi (arrow) are related to the orientation of the surrounding fibres (double-headed arrow). (d) Transmitted natural light. Semi-thin vertical section of partially demineralised scales. Toluidine blue staining. The organic matrix is stained in grey and the mineral remnants are black. (e) Nomarski interference optical micrograph. Semi-thin vertical section of a demineralised scale showing the abundant fractures. (f) Nomarski interference optical micrograph. Semi-thin vertical section of a demineralised scale showing the rippled surface of the basal plate. Micro-organisms, probably bacteria, are visible (arrow). (g) TEM. Demineralised scale. Basal plate. Closely packed fibrils are roughly parallel to each other and are connected by bridges. Insert: detail of bridges connecting two adjacent fibrils (arrows). (h) TEM. Partially demineralised scale. Some fibrils show a discernible periodic striation (arrows).

Fig. 3. *Eusthenopteron foordi*. Écailles. (a) Lumière naturelle transmise. Lame mince. Coupe transversale de la plaque basale montrant deux couches superposées : la couche externe (el) et la plaque basale stratifiée (bp). (b) Lumière polarisée. Coupe transversale montrant des détails de l'empilement des couches formant la plaque basale. (c) Lumière naturelle transmise. Coupe épaisse frontale d'épon après déminéralisation. L'organisation de l'écaille est bien préservée. La forme des lacunes ostéocytaires et des canaliculi (flèche) sont en relation avec l'orientation des fibrilles (flèche à deux têtes). (d) Lumière naturelle transmise. Coupe semi-fine partiellement déminéralisée et colorée par le bleu de toluidine. Coupe transversale d'écaille. La matrice organique est colorée en gris, alors que les dépôts minéraux apparaissent en noir. (e) Photo par interférence optique Nomarski. Coupe semi-fine transversale d'une écaille déminéralisée montrant de nombreuses fractures. (f) Nomarski. Coupe semi-fine transversale d'une écaille déminéralisée montrant l'aspect ondulé de la surface de la plaque basale. Des micro-organismes, probablement des bactéries, sont visibles (flèche). (g) MET. Écaille déminéralisée. Plaque basale. Des fibrilles étroitement associées et approximativement parallèles les unes aux autres, sont réunies par des ponts. Encart : Détail des ponts réunissant des fibrilles adjacentes (flèches). (h) MET. Écaille partiellement déminéralisée. Certaines fibrilles montrent une striation périodique (flèches).

canals that housed blood vessels, observed only in cortical bone. At the ultrastructural level, the extracellular matrix is composed of a network of very thin fibrils (Fig. 4e). Thin sections of the cortical bone show that blood vessel canal sections are surrounded by rings of more electron-dense material corresponding to the blue stained rings observed in light microscopy. This electron-dense material contains elongated mineral crystals whose size and morphology differ from those of hydroxyapatite crystallites in bone. Nevertheless, the crystals are approximately oriented along the axes of the fibrils (Fig. 4f).

Triassic bones were examined in the temnospondyls *Tupilakosaurus wetlugensi* and *Eryosuchus garjaino*, in both cases using ribs. Demineralisation has not dissolved the mineral that remains in some areas of the ground sections in samples of *T. wetlugensis* (Figs. 5a_1, a_2) and *E. garjainov* (Figs. 5 h_1, h_2). Ground sections of the rib of *T. wetlugensis* show that the axes of the abundant osteocyte lacunae are parallel to each other (Fig. 5b_1) and to the bundles of closely packed fibrils (Fig. 5b_2). Semi-thin sections of the ribs of *T. wetlugensi* show two distinct areas separated by a clear-cut line (Fig. 5c). A completely demineralised area contains abundant osteocyte lacunae. The other area, stained with toluidine blue, is partially mineralised (Fig. 5c). These two parts differ also at the ultrastructural level. The demineralised area is composed of a fairly dense amorphous material. Ribbons are made of a dense meshwork (Fig. 5d). In the partially mineralised area,

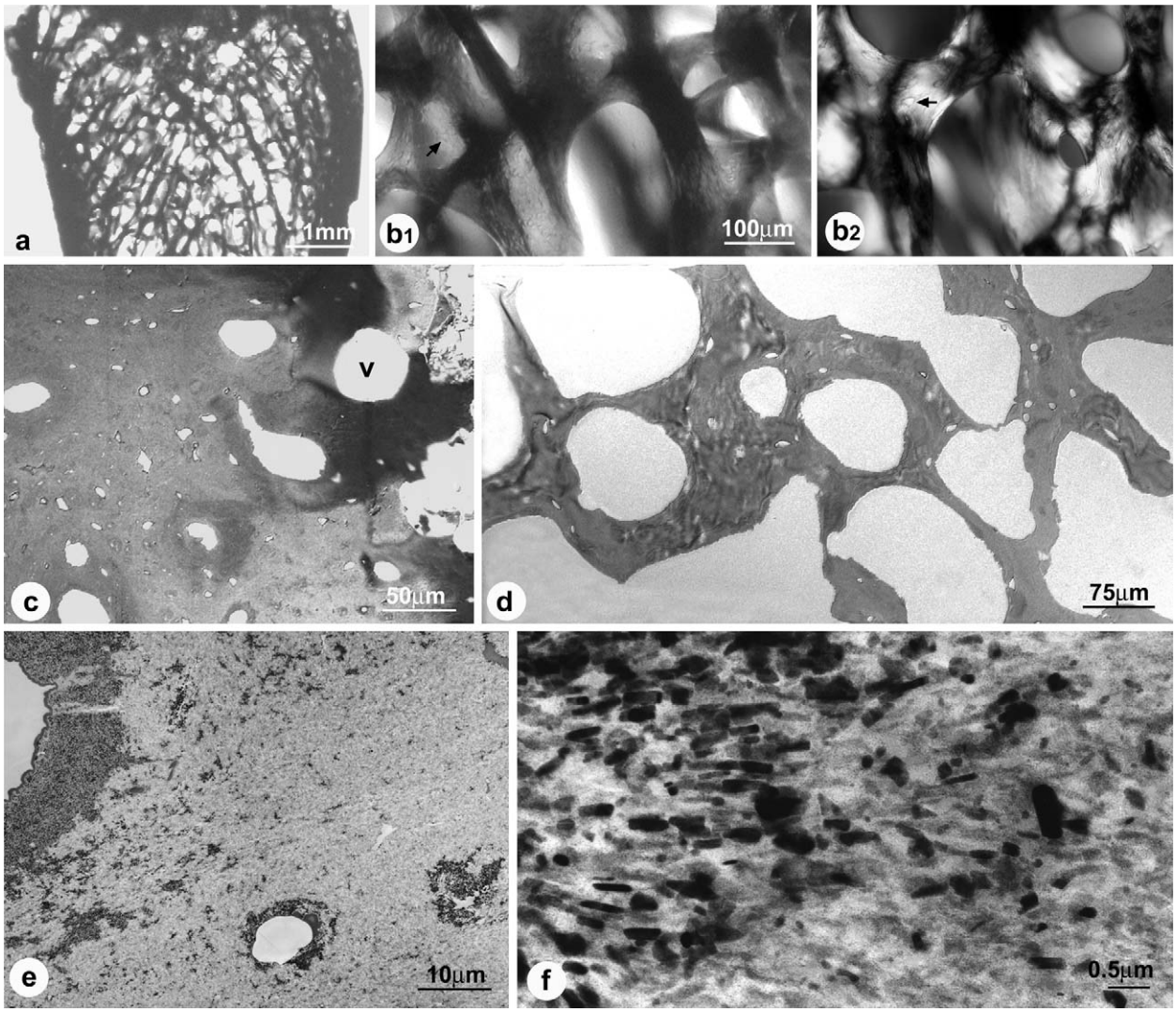

Fig. 4. *Captorhinus aguti* femur. Permian. (a) Transmitted natural light. Longitudinal Epon ground section of the femur after demineralisation. (b) Detail of the spongiosa in transmitted natural light (b_1) and polarised light (b_2) The spongiosa shows well-preserved trabeculae and osteocyte lacunae (arrow). (b_2) Polarised light shows lamellar bone in the trabeculae. (c) Transmitted natural light. Semi-thin section. Toluidine blue staining. Abundant osteocyte lacunae are observed. Dense material showing a great affinity for toluidine blue is located around the vessels (v). (d) Transmitted natural light. Semi-thin section at the level of the trabeculae. Toluidine blue staining. (e) TEM. Same area as in (c). An electron-opaque material surrounds the empty spaces formerly occupied by the vessels. (f) TEM. Detail of the electron-opaque areas. Parallelepipedic crystals are coaligned with fibrils.

Fig. 4. *Captorhinus aguti.* Fémur. Permien (a) Lumière naturelle transmise. Lame mince d'une coupe longitudinale du fémur incluse dans l'épon après déminéralisation. (b) Détail de la spongiosa en lumière naturelle transmise (b_1) et lumière polarisée (b_2). Les trabécules de la spongiosa sont bien conservés. Des lacunes ostéocytaires sont visibles (flèche). (c) Lumière naturelle transmise. Coupe semi-fine. Bleu de toluidine. Les logettes ostéocytaires sont nombreuses. Un matériel dense montrant une grande affinité pour le bleu de toluidine est situé autour d'espaces correspondant aux vaisseaux sanguins (v). (d) Lumière naturelle transmise. Coupe semi-fine au niveau des trabécules, colorée au bleu de toluidine. (e) MET. Même région que (c). Un matériel opaque aux électrons entoure les espaces occupés par les vaisseaux sanguins sur le vivant. (f) MET. Détail des zones opaques aux électrons. Des cristaux ayant une forme de parallélépipède ont la même orientation que les fibrilles auxquelles ils sont associés.

the fibrils oriented approximately parallel to each other form a network associated with crystals (Fig. 5e). The closely packed fibrils form bundles (Fig. 5f) within which a weak striation is discernable (Fig. 5 g). The fibrils are interconnected by irregularly-spaced rods.

The ground sections of *E. garjainov* show abundant osteocyte lacunae randomly distributed within the matrix (Fig. 5i_1) where polarised light does not show a peculiar organisation (Fig. 5i_2). Toluidine blue stains only the demineralised part of the semi-thin section; the unstained areas are still at least partially mineralised (Fig. 5j). Empty spaces correspond to the vessels (Fig. 5j). At the ultrastructural level, the matrix appears to be made of a network of electron-dense fibrils (Fig. 5k). The fibrils show an irregular banding. They appear to contain small crystals (Fig. 5l).

The humerus of the Jurassic dinosaur *Lapparentosaurus madagascariensis* differs from the geologically much older *C. aguti* femur. Indeed, the humerus of

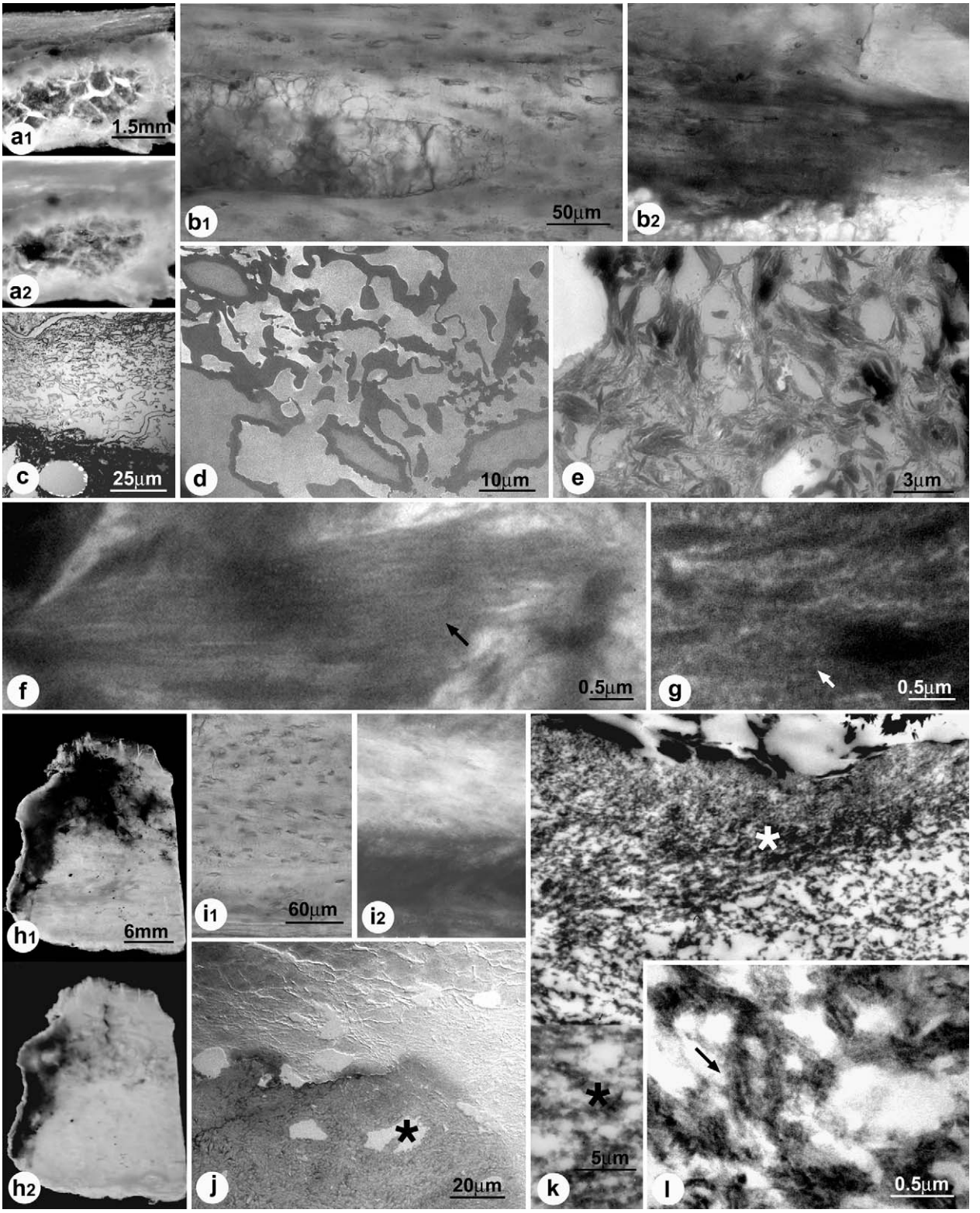
a1
1.5mm
a2
b1
50μm
b2
c
25μm
d
10μm
e
3μm
f
0.5μm
g
0.5μm
h1
6mm
h2
i1
60μm
i2
j
20μm
k
5μm
l
0.5μm

Fig. 5.

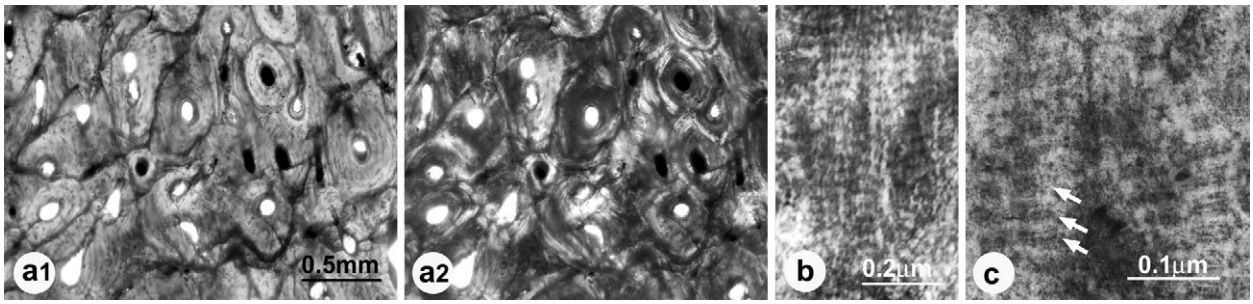

Fig. 6. Ground section. Cross-section of the diaphysis in *Lapparentosaurus madascariensis*. Humerus. Jurassic. Transmitted natural (a_1) and polarised light (a_2). Several generations of secondary osteons overlap each other. (b) TEM. Fibrils oriented in parallel to each other show a periodic striation similar to the one of modern collagen. (c) TEM. Electrolucent and electron-dense zones causing the periodic striation of the fibrils are themselves made of successive electron-lucent and electron dense bands (arrows) as in fibrils of extant collagen.
Fig. 6. Lame mince. Coupe transversale de la diaphyse de l'humérus de *Lapparentosaurus madascariensis*. Jurassique. Lumière naturelle transmise (a_1) et lumière polarisée (a_2). Plusieurs générations d'ostéones secondaires se chevauchent les uns les autres. (b) MET. Des fibrilles parallèles les unes aux autres ont une striation périodique qui s'apparente à celle du collagène actuel. (c) MET. Les zones opaques aux électrons et les zones transparentes aux électrons qui forment la striation périodique sont elles-mêmes constituées de bandes claires et sombres aux électrons, comme dans les fibrilles de collagène actuel.

L. madagascariensis is much denser and is composed of a secondary haversian bone where osteons overlap each other as observed in ground sections (Figs. 6

a_1, a_2). Examination at the ultrastructural level reveals that the matrix contains patches where striated fibrils oriented in parallel (Fig. 6b) are organised in bundles as in modern osseous tissue. The periodic striation of the fibrils is due to sequences of electron-dense and electron-lucent zones that are themselves made of thin striations as in fibrils of extant collagen (Fig. 6c).

5. Discussion

The present preliminary study, although it concerns only a few specimens ranging in age from Devonian to Jurassic, shows that organic residues are frequently preserved after at least a partial or a complete demineralisation of fossil bone ground sections. The ultrastructural aspects of these organic residues suggest that they represent the remains of bone organic matrix rather than the bacterial biofilms described by Kaye et al. (2008) at the surface of fossil samples. Biofilms contain pyrite framboids (Maclean et al., 2008) that were not observed in our samples. Indeed, TEM examination carried out in the present study shows that reasonably well-preserved fibrils are identified within all specimens. However, the characteristic banding of type I collagen is distinguishable in few of the studied specimens. Pawlicki et al. (1966), Doberenz and Wickoff (1967), and Schweitzer et al. (2005, 2007) stated that collagen in fossil bone lose its ability to be stained and its characteristic banding, but our observations show that collagen in fossil bone can frequently be stained and retains part of the banding pattern. Fibrils show striations in the scales of the Devonian sarcopterygian *E. foordi* and in the humerus of the Jurassic dinosaur *L. madagascariensis*. The banding observed in *L. madagascariensis* resembles that of

Fig. 5. Ribs of the Triassic temnospondyls *Tupilakosaurus wetlugensis* (a–g) and *Eryosuchus garjainov* (h–l). (a_1) Transmitted natural light. Ground section before demineralisation showing two parts, one of which is composed of compact bone surrounding a central spongiosa. (a_2) The same ground section after demineralisation. (b) Detail of the compact bone in ground section observed with natural transmitted light (b_1) and with polarised light (b_2). The abundant osteocyte lacunae (b_1) have their axes roughly oriented in parallel with the fibrillar bundles (b_2). (c) Transmitted natural light. Semi-thin section. Toluidine blue staining reveals two areas: one composed of a loose meshwork, and another, denser and intensively stained region. (d) TEM. The loose meshwork contains an amorphous material of variable density. (e) TEM. The dense part contains a fibrillar network within which mineral crystals are entrapped. (f) TEM. Fibrils are closely packed in the bundles (arrow). (g) TEM. Detail of a bundle within which the fibrils show a weak striation (arrow). (h_1) Transmitted natural light. Ground section before demineralisation shows heterogeneous opacity. (h_2). The same ground section after demineralisation. Large areas of sample lost their opacity during demineralisation. (i) Ground section. Detail of the organisation within the bone. (i_1) Transmitted natural light showing the random distribution of osteocyte lacunae. (i_2) Polarised light. The fibrils show no preferential direction. (j) Transmitted natural light. Semi-thin section. Toluidine blue staining. Only one part of the section is stained. Holes (asterisk) correspond to vessels. (k) TEM. Fibrils are organised in a dense (white asterisk) or loose (black asterisk) network. (l) TEM. Detail of fibril structure (arrow).
Fig. 5. Côtes des temnospondyles triasiques *Tupilakosaurus wetlugensis (a–g)* et *Eryosuchus garjainov* (h–l). (a_1) Lumière naturelle transmise. Lame mince avant déminéralisation montrant deux régions, l'une composée d'os compact bordant une spongiosa centrale. (a_2) Même lame mince après déminéralisation. (b) Lame mince. Détail de l'os compact. (b_1) Lumière naturelle transmise. (b_2) Lumière polarisée. Les nombreuses logettes ostéocytaires (b_1) ont leur grand axe orienté parallèlement à celui des faisceaux fibrillaires (b_2). (c) Lumière naturelle transmise. Coupe semi-fine. Bleu de toluidine. Deux régions diffèrent par leur affinité pour le colorant. L'une est composée d'un réseau peu dense et l'autre, d'un réseau plus dense et plus vivement coloré. (d) MET. Un réseau lâche est constitué d'un matériel amorphe plus ou moins dense. (e) MET. La partie plus dense contient un réseau fibrillaire au sein duquel les cristaux sont inclus. (f) MET. Les fibrilles forment des faisceaux compacts (flèche). (g) MET. Détail d'un faisceau composé de fibrilles montrant une discrète striation (flèche). (h_1) Lumière naturelle transmise. Lame mince avant déminéralisation montrant une opacité hétérogène. (h_2) Même lame mince après déminéralisation. Des régions plus étendues de la lame mince ont perdu leur opacité. (i) Lame mince. Détail de l'organisation de l'os. (i_1) Lumière naturelle transmise. Les logettes ostéocytaires sont réparties sans ordre. (i_2) Lumière polarisée. Les fibrilles n'ont pas de direction préférentielle. (j) Lumière naturelle transmise. Coupe semi-fine. Coloration par le bleu de toluidine. Seule une partie de coupe est colorée. Les espaces vides (astérisque) correspondent aux vaisseaux sanguins. (k) MET. Des fibrilles forment un réseau dense (astérisque blanche) ou un réseau lâche (astérisque noire). (l) MET. Détail de la structure des fibrilles (flèche).

the fibrils of modern collagen and it is in the range of the characteristic 64 nm banding, as reported by Rimblot-Baly et al. (1995). Differences in the banding between the fossil and the extant material noted by Wickoff et al. (1963) and Shackleford and Wickoff (1964) can be related, on one hand, to a change in the collagen molecule and, on the other hand, to the processing involved in the preparation of the fossil bone for electron microscopical examination. For comparison of the banding in fossils from different sources, the samples have to be prepared under identical conditions and viewed in the same microscope. The electron microscope itself must be calibrated for a valid measurement of the banding of material (Armstrong et al., 1983). Such measurements are not in the scope of the present study, the samples have been prepared under identical conditions, but they have been examined with two different microscopes.

The fibrils are often associated with mineral crystallites, as observed in our partially demineralised samples of fossil bones. Depending of their size, the crystallites are inserted within the fibril, as in *E. foordi*, *T. wetlugensis,* and *Eryosuchus garjaini*, or their axes are oriented in the same direction as the fibrils, as in *Captorhinus aguti*. It has been shown that in fossil bone, crystallites retain the orientation of the bone crystals although they are larger (Dumont et al., 2011; Hubert et al., 1996; Newesely, 1989; Trueman et al., 2008; Wess et al., 2001; Zocco and Schwartz, 1994).

In the present work, fossil bone preservation does not appear to depend on geological age and may instead reflect the structure of fossil bone, particularly the arrangement and density of the collagen fibrils. Indeed, the bones of *Eusthenopteron* and *Lapparentosaurus* share a twisted plywood-like structure in which collagen fibrils are very closely packed (Giraud-Guille, 1988; Giraud et al., 1978). TEM analysis of the postcranial dermal skeleton of *E. foordi* did not enable ultrastructural observations of collagen fibrils in other elements such as lepidotrichia or enlarged scales (Zylberberg et al., 2010). The ultrastructural preservation of the twisted plywood-like structure of the basal plate despite cracks and the presence of micro-organisms may have been facilitated by high density of the fibrils within the plies. In the plies where the fibrils are closely packed, abundant bridges connecting fibrils are preserved, even if these bridges may have formed during fossilisation and may not correspond to the bridges composed of glycosaminoglycans and glycoproteins found in fresh osseous tissues (Fawcett, 1994; Rossert and de Combrugghe, 2002). The fibrils show an occasional striation evoking that of the type I collagen of bone. In *L. madagascariensi*, TEM reveals an ultrastructural striation along the well-preserved fibrils similar to that of modern collagen. Conversely, only a low concentration of peptide residues has been identified in bone from the same area by biochemical analyses (Rimblot-Baly et al., 1995). It has already been noted that the appearance of collagen fibrils under electron microscopy does not always reflect the survival of intact protein components since there is now evidence of subtle degradation of collagen molecules that remain structurally intact (Armstrong and Tarlo, 1966; Armstrong et al., 1983; Nielsen-Marsh, 2002). Long-term preservation of organic macromolecules may occur where recrystallisation rates are particularly fast (Trueman et al., 2008). The rate of collagen degradation in bone is slow because its mineral component protects the collagen of the matrix by preventing helical expansion, which precedes fibril degradation.

Acknowledgments

The authors are greatly indebted to Pr Armand de Ricqlès for inspiring this research and for loaning the specimens of *L. madagascariensis* and *C. aguti*. We thank Mr. Sylvain Desbiens and Ms Johanne Kerr for loaning us the specimens of *Eusthenopteron* and for permission to section them, Dr. Philippe Janvier (MNHN, Paris, France) for providing us with some specimens and for his help to contact the Parc de Miguasha. We thank Pr. Robert Reiz (Vertebrate Paleontology, University of Toronto, Canada) for the loan of specimens of Dissordophoidea, Pr Mikhail Shinkin (Paleontological Institute, Moscow, Russia) for the loan of *M. exiguus*, *E. garjainovi*, *T. wetlugensis* and Dr. Jean-Sébastien Steyer (MNHN, Paris, France) for the loan of *O. frossardi* and for their permission to section these specimens. We are grateful to Françoise Allizard (CNRS, UPMC, Paris, France), Christiane Chancogne (MNHN, Paris, France) for their technical assistance respectively for TEM and SEM, and to Michel Lemoine (MNHN, Paris, France), Marie-Madeleine Loth (CNRS, UPMC, Paris, France) and Hayat Lamrous (Collège de France, UPMC, Paris) for ground sections. TEM observations were carried out in The Department of Electron Microscopy, IFR Biologie Intégrative, CNRS and UPMC, Paris, France.

References

Armitage, M., 2001. Scanning electron microscope study of mummified collagen fibers in fossil *Tyrannosaurus rex* bone. CRS Q. 38, 61–66.
Armstrong, W.G., Tarlo, L.B.H., 1966. Amino-acid components in fossil calcified tissues. Nature 210, 481–482.
Armstrong, W.G., Halstead, L.B., Reed, F.B., Wood, L., 1983. Fossil proteins in vertebrate calcified tissues. Phil. Trans. R. Soc. Lond. B 301, 301–343.
Bulanov, V.V., 2003. Evolution and systematics of seymouriamorph parareptiles. Paleont. J. 37, S1–S105.
Collins, M.J., Nielsen-Marsh, C.M., Hiller, J., Smith, C.I., Roberts, J.P., Prigodich, R.V., Wess, T.J., Csapò, J., Millard, A.R., Turner-Walker, G., 2002. The survival of organic matter in bone: a review. Archaeometry 44, 383–394.
Collins, M.J., Riley, M.S., Child, A.M., Turner-Walker, G., 1995. A basic mathematical simulation of the chemical degradation of ancient collagen. J. Archaeol. Sci. 22, 175–183.
Doberenz, A.R., Wickoff, W.G., 1967. Fine structure in fossil collagen. Proc. Natl. Acad. Sci. U S A 57, 539–541.
Dumont, M., Pyzalla, A., Kosta, A., Borbély, A., 2011. Characterization of Sauropod bone structure. In: Klein, N., Remes, K., Gee, C.T., Sander, P.M. (Eds.), Biology of Sauropod Dinosaurs: understanding the life of giants. Indiana University Press, Bloomington, pp. 149–169.
Eglinton, G., Logan, G.A., 1991. Molecular preservation. Phil. Trans. R. Soc. Lond. B. 333, 315–328.
Fawcett, D.W., 1994. Bloom and Fawcett. A textbook of histology, 12th ed. Chapman and Hall, New York, London, 964 p.
Fernández-Jalvo, Y., Sanchez-Chillón, B., Andrews, P., Fernández-López, S., Alcalá Martínez, L., 2002. Morphological taphonomic transformations of fossil bones in continental environments, and repercussions on their chemical composition. Archaeometry 44, 353–361.
Francillon-Vieillot, H., de Buffrénil, V., Castanet, J., Géraudie, J., Meunier, F.J., Sire, J.Y., Zylberberg, L., de Ricqlès, A., 1990. Microstructure and mineralization of vertebrate skeletal tissues. In: Carter, J.G. (Ed.), Biomineralization: patterns and evolutionary trends. Van Nostrand Reinold, New York, pp. 471–530.

Giraud, M.M., Castanet, J., Meunier, F.J., Bouligand, Y., 1978. The fibrous structure of coelacanth scales: atwisted "plywood". Tissue Cell 10, 671–686.
Giraud-Guille, M.M., 1988. Twisted plywood architecture of collagen fibrils in human compact bone osteons. Calcif. Tissue Intern. 42, 167–180.
Glimcher, M.J., Krane, S.M., 1968. The organisation and structure of bone and the mechanism of calcification. In: Ramachandran, G.N., Bould, B. (Eds.), Treatise of collagen, 2. Academic Press, London, pp. 67–251.
Gradstein, F.M., Ogg, J.G., Smith, A.G., 2004. A Geologic Time Scale 2004. Cambridge University Press, Cambridge, 589 p.
Hancox, N.M., 1972. Biology of Bone. Cambridge University Press, Cambridge, p. 6–17.
Hubert, J.F., Panish, P.T., Chure, D.J., Prostak, K.S., 1996. Chemistry, microstructure, petrology, and diagenic model of Jurassic dinosaur bones, Dinosaur National Monument, Utah. J. Sedimentary Res. 66, 531–547.
Isaacs, W.A., Little, K., Currey, J.D., Tarlo, L.B.H., 1963. Collagen and a cellulose-like substance in fossil dentine and bone. Nature 197, 192.
Jans, M.M.E., Kars, H., Nielsen-Marsh, C.M., Smith, C.I., Nord, A.G., Arthur, P., Earl, N., 2002. *In situ* preservation of archaeological bone: a histological study within a multidisciplinary approach. Archaeometry 44, 343–352.
Josse, S., Moreau, T., Laurin, M., 2006. Stratigraphic tools for Mesquite. http://mesquiteproject.org/packages/stratigraphicTools/.
Kaye, T.G., Gaugier, G., Sawlowicz, Z., 2008. Dinosaurian soft tissues interpreted as bacterial biofilms. Plos ONE 3, 1–7.
Laurin, M., 1998. A reevaluation of the origin of pentadactyly. Evolution 52, 1476–1482.
Laurin, M., 2008. Systématique, paléontologie et biologie évolutive moderne : l'exemple de la sortie des eaux des vertébrés. Ellipses, Paris, 176 p.
Laurin, M., Anderson, J.S., 2004. Meaning of the name Tetrapoda in the scientific literature: an exchange. Syst. Biol. 53, 68–80.
Laurin, M., Reisz, R.R., 1995. A reevaluation of early amniote phylogeny. Zool. J. Linn. Soc. 113, 165–223.
Laurin, M., Soler-Gijón, R., 2006. The oldest known stegocephalian (Sarcopterygii: Temnospondyli) from Spain. J. Vert. Paleont. 26, 284–299.
Lees, S., 1989. Some characteristics of mineralised collagen. In: Hukins, D.W. (Ed.), Calcified tissue: topics in molecular and structural biology. Macmillan, London, pp. 153–173.
Lyson, T.R., Bever, G.S., Bhullar, B.A.S., Joyce, W.G., Gauthier, J.A., 2010. Transitional fossils and the origin of turtles. Biol. Lett. 6, 830–833.
Maclean, L.C.W., Tyliszczak, T., Gilbert, P.U.P.A., Zhou, D., Pray, T.J., Onstott, Southam, G., 2008. A high-resolution chemical and structural study of framboidal pyrite formed within a low tempreature bacterial biofilm. Geobiology 6, 471–480.
Maddison, W.P., Maddison, D.R., 2010. Mesquite: a modular system for evolutionary analysis. Version 2.74. http://mesquiteproject.org.
Marjanovic, D., Laurin, M., 2009. The origin(s) of modern amphibians: a commentary. Evol. Biol. 36, 336–338.
Meunier, F.J., 1984. Spatial organization and mineralization of the basal plate of elasmoid scales in osteichthyans. Am. Zool. 24, 953–964.
Newesely, H., 1989. Fossil bone apatite. Appl. Geochem. 4, 233–245.
Nielsen-Marsh, C., 2002. Biomolecules in fossil remains. The Biochemist, 12–14.
Pawlicki, R., 1985. Metabolic pathways of the fossil dinosaur bones. Part V. Morphological differentiation of osteocyte lacunae and bone canaliculi and their significance in the system of extracellular communication. Folia Histochem. Cytochem. 23, 165–174.
Pawlicki, R., Korbel, A., Kubiac, H., 1966. Cell, collagen fibrils and vessels in dinosaur bone. Nature 211, 1502–1503.
Rieppel, O., Reisz, R.R., 1999. The origin and early evolution of turtles. Annu. Rev. Ecol. Syst. 30, 1–22.
Rimblot-Baly, F., de Ricqlès, A., Zylberberg, L., 1995. Analyse paléohistologique d'une série de croissance partielle chez *Lappentosaurus madagascariensis* (Jurassique moyen) : essai sur la dynamique de croissance d'un dinosaure sauropode. Ann. Paléontol. 81, 49–86.
Robey, G., 2002. Bone matrix proteoglycans and glycoproteins. In: Bilezikian, J.P., Raisz, L.G., Rodan, G.A. (Eds.), Principles of bone biology, 1. Academic Press, San Diego, pp. 225–237.
Rossert, J., de Combrugghe, B., 2002. Type I collagen: structure, synthesis and regulation. In: Bilezikian, J.P., Raisz, L.G., Rodan, G.A. (Eds.), Principles of bone biology, 1. Academic Press, San Diego, pp. 189–210.
Ruta, M., Coates, M.I., 2007. Dates, nodes and character conflict: addressing the lissamphibian origin problem. J. Syst. Palaeontol. 5, 69–122.
Schweitzer, M.H., Avci, R., Collier, T., Goodwin, M.B., 2008. Microscopic, chemical, and molecular methods for examining fossil preservation. C. R. Palevol 7, 159–184.
Schweitzer, M.H., Wittmeyer, J.L., Horner, J.R., Toporski, J.K., 2005. Soft tissue vessels and cellular preservation in *Tyrannosaurus rex*. Science 307, 1952–1955.
Schweitzer, M.H., Wittmeyer, J.L., Horner, J.R., 2007. Soft tissue and cellular preservation in vertebrate skeletal elements from the Cretaceous to the present. Proc. R. Soc. B 274, 183–197.
Scott, J.E., Kyffin, T.W., 1978. Demineralization in organic solvents by alkylammonium salts of ethylenediaminetetra-acidic acid. Biochem. J. 169, 697–701.
Shackleford, J.M., Wickoff, W.G., 1964. Collagen in fossil teeth and bones. J. Ultrastruct. Res. 11, 173–180.
Trueman, C.N., Martill, D.M., 2002. The long-term survival of bone: the role of bioerosion. Archaeometry 44, 371–382.
Trueman, C.N., Palmer, M.R., Field, J., Privat, K., Ludgate, N., Chavagnac, V., Eberth, D.A., Cifelli, R., Rogers, R.R., 2008. Comparing rates of recrystallisation and the potential for preservation of biomolecules from distribution of trace elements in fossil bones. C. R. Palevol 7, 145–158.
Van der Rest, M., 1991. The collagen of bone. In: Hall, B.K. (Ed.), Bone, 3. CRC Press Inc., Boca Raton, pp. 187–237.
Weiner, S., Traub, W., 1986. Organization of hydroxyapatite crystals within collagen fibrils. FEBS Lett. 206, 262–266.
Wess, T., Alberts, I., Hiller, J., Drakopoulos, M., Chamberlain, A.T., Collins, M., 2001. Microfocus small angle X-ray scattering reveals structural features in archaeological bone samples: detection of changes in bone mineral habit and size. Calcif. Tissue Inter. 70, 103–110.
Wickoff, R.W.G., Wagner, E., Matter, P., Doberenz, A.R., 1963. Collagen in fossil bone. Proc. Natl. Acd. Sci. U. S. A. 50, 215–218.
Yates, A.M., Warren, A., 2000. The phylogeny of the 'higher' temnospondyls (Vertebrata: Choanata) and its implications for the monophyly and origins of the Stereospondyli. Zool. J. Linn. Soc. 128, 77–121.
Zocco, T.G., Schwartz, H.L., 1994. Microstructural analysis of bone of the sauropod dinosaur *Seismosaurus* by transmission electron microscopy. Palaeontology 37, 493–503.
Zylberberg, L., Meunier, F.M., Laurin, M., 2010. A microanatomical and histological study of the postcranial dermal skeleton in the Devonian sarcopterygian *Eusthenopteron foordi*. Acta Palaeontol. Polonica 55, 459–470.